

## Probe Diffusion in Polymer Solutions in the Dilute/Semidilute Crossover Regime. 2. Polyelectrolytes

E. C. Cooper,<sup>†</sup> P. Johnson, and A. M. Donald\*

*Cavendish Laboratory, Department of Physics, University of Cambridge, Madingley Road, Cambridge CB3 0HE, U.K.*

*Received February 18, 1991; Revised Manuscript Received May 6, 1991*

**ABSTRACT:** The Stokes-Einstein relationship has been tested for the motion of polystyrene latex particles moving through two different polyelectrolytes, sodium poly(styrene sulfonate) and poly(L-lysine) (PLL). The motion of the particles, which are negatively charged, through sodium poly(styrene sulfonate) solutions shows deviations corresponding to a greater slowing down of the particles than expected from measurements of the macroscopic viscosity. This behavior is similar to that seen for a neutral polymer and is thought to be due to the effect of tails in the adsorbed layer. In contrast, PLL initially showed an apparent speeding up of the particles. However, as the concentration of PLL was raised, a steep increase in the ratio of the viscosity calculated from sedimentation to that directly measured was found. This behavior is attributed to a change in the conformation of the adsorbed layer from a rather flat configuration at low concentrations to a much more extended one at high concentrations, when interchain screening of charges allows the molecule to become more flexible.

### Introduction

In recent years, the diffusion of small particles through polymer solutions has been extensively studied as a means of probing the nature of the mesh in the entangled solution.<sup>1-14</sup> In general, these studies have examined deviations of the diffusion coefficient ( $D$ ) from that expected from the Stokes-Einstein relation

$$D = \frac{k_B T}{6\pi\eta R} \quad (1)$$

In this equation,  $\eta$  is the solvent viscosity,  $R$  is the radius of the particle,  $k_B$  is Boltzmann's constant, and  $T$  is the absolute temperature. However, the details of these deviations do not seem to be universal, although in practice much of the data can be reduced to fit a stretched exponential form as proposed by Phillies and co-workers:<sup>2-9</sup>

$$D/D_0 = \exp(-AC^\nu I^\beta R^\delta) \quad (2)$$

where  $D_0$  is the diffusion coefficient in pure solvent,  $A$  is a constant, and  $I$  is the ionic strength of the solution. The indices  $\nu$ ,  $\beta$ , and  $\delta$  are determined experimentally, with most data supporting a value of  $\nu$  between 0.5 and 1. Most of the work indicates a speeding up of the particles relative to that expected from eq 1. Given that the polymer solution above the overlap concentration ( $C^*$ ) can be characterized in terms of an average mesh size ( $\xi$ ),<sup>15-19</sup> this speeding up has been interpreted in terms of the particles being able to slip through the mesh of the entangled polymer solution when  $R < \xi$ . However, it was also found that the effect continued beyond the point where the particle radius exceeded the mesh size.

Much of the work on probe diffusion has been carried out on polyelectrolytes. For such systems, the situation is complicated by the nontrivial evaluation of  $\xi$ . For neutral, flexible polymers,  $\xi$  is simply related to the concentration and the radius of gyration,  $R_g$ , of the polymer by a scaling relation<sup>19</sup>

$$\xi = R_g (C^*/C)^n \quad (3)$$

where the exponent  $n$  is 0.75 to satisfy the requirement

that  $\xi$  is independent of molecular weight. For polyelectrolytes, there are other length scales of importance that enter into the expression for  $\xi$ . Specifically, Odijk<sup>20</sup> has written  $\xi$  as

$$\xi = L_t^{-1/4} \kappa^{1/4} (aC)^{-3/4} \quad (4)$$

where  $L_t$  is the total persistence length of the polyelectrolyte chain,  $\kappa$  is the Debye-Hückel constant, and  $a$  is the separation between charges along the chain. However, at zero or low salt content, as the concentration of polymer chains increases, screening of one by others will become increasingly important, leading to a modification of the concentration dependence implied by eq 4, which was derived neglecting the influence of other chains on the configuration of a given chain.

A second complication in interpreting the measured diffusion coefficients in relation to the Stokes-Einstein equation is the possibility of adsorption. This has been recognized by various authors but has usually been treated as simply leading to an increase in the effective particle size.<sup>5,6,12</sup> However, a recent study on the system poly(ethylene oxide) (PEO)-polystyrene (PS) latex-water has shown that the presence of long tails in the adsorbed layer can have a dramatic effect, leading to a significant *slowing down* of the PS particles at moderate PEO concentrations.<sup>14</sup> This can be interpreted in terms of the local concentration around the latex spheres, becoming appreciably different from the bulk concentration due to the tails entangling with the polymer chains in solution, and hence a different effective viscosity will be operative. Figure 1 shows a typical curve for the PEO system. In this figure, the data are plotted in terms of the ratio of the observed effective viscosity in sedimentation,  $\eta_e$ , to the macroscopically determined viscosity,  $\eta_m$ . A value for this ratio of unity implies the Stokes-Einstein equation is obeyed; values greater than 1 imply the particle is slowed down as compared with the Stokes equation. When 0.01% Triton is added to the system, the deviations become much less marked<sup>14</sup> due to the adsorption of PEO being almost completely suppressed. For many polyelectrolytes, which frequently adsorb in a rather flat configuration,<sup>12,21-24</sup> the effect of tails may not be significant, and it is probably for this reason that such slowing down has not previously been observed for polyelectrolytes (which have served as the focus for most of the work on probe diffusion).

<sup>†</sup> Present address: BP Research Centre, Sunbury-on-Thames, Middlesex, U.K.

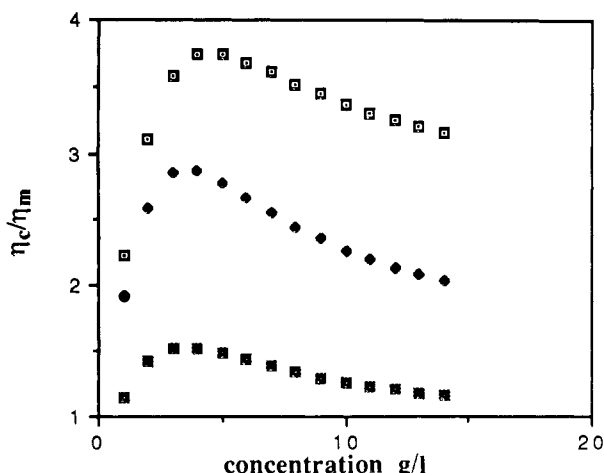


**Figure 1.** Plot of the ratio of the calculated viscosity to the macroscopically measured viscosity as a function of PEO (with molecular weight of 615 000) concentration for PS latex particles; probe radius 32 nm ( $\square$ ), 65 nm ( $\blacklozenge$ ), and 447 nm ( $\blacksquare$ ).

In this paper, the results are presented on the motion of PS particles through two polyelectrolytes, sodium poly(styrene sulfonate) (NaPSS) and poly(L-lysine) (PLL). These two polymers are oppositely charged, but both are known to adsorb to negatively charged PS latex spheres. The possible effects of the adsorbed layer are examined in light of the results on PEO. In addition, the effects of probe particle size and polymer molecular weight and a brief comparison of the results from sedimentation data and dynamic light scattering are presented.

Furusawa et al.<sup>21</sup> have studied the adsorption behavior of poly(L-lysine) at the negatively charged polystyrene latex–water interface. They found that the conformation of PLL in the bulk persists in the adsorbed state. Adsorption of a polyelectrolyte onto a charged surface is usually very rapid and irreversible. According to Furusawa et al.'s measurements of the electrophoretic mobility of the PLL-coated particles, a pronounced charge reversal of the original particles occurred at the saturation adsorption of PLL and this (positive) charge was numerically greater than the original negative charge on the latex surface. It is known that the narrow flocculation range (at low pH) does not correspond to the polymer concentration for making an effective interparticle bridge but does correspond to the charge neutralization. The concentration range of PLL used in these experiments extended to well above that required for full surface coverage of the particles.<sup>21</sup> Both the work of Furusawa et al.<sup>21</sup> and that of Bonekamp et al.<sup>22</sup> indicate that for PLL at pH's below that of the coil–helix transition (pH  $\sim$  10.6) adsorption onto PS latices is in a rather flat configuration with few tails.

Cosgrove et al.<sup>24</sup> have found that (negatively charged) NaPSS also usually adsorbs onto highly negative polystyrene latex particles in a relatively flat configuration at low ionic strengths, with the hydrodynamic layer thickness,  $\delta_H$ , small compared with neutral polymers of similar molecular weight and adsorbed amount, indicating that the tails were relatively short ( $\delta_H \sim$  4 nm for NaPSS of molecular weight 74 000 and  $\sim$  30 nm for 780 000 molecular weight). However, for weakly charged particles such as those used in this study, the layer thickness may become substantial (e.g., 40 nm for NaPSS of molecular weight 74 000), suggestive of more extensive tail formation.<sup>24</sup> It should be mentioned, however, that estimates of  $\delta_H$  from dynamic light scattering may be unreliable since adsorption may be accompanied by aggregation, which tends to be

**Table I**  
Characteristics of the Various PLL Samples

PLL MW	$M_w/M_n$	$C^*/\text{g L}^{-1}$	$C/C^*$	
			at min	at $\eta_c/\eta_m = 1$
52 000	1.17	2.3	6.05	9.03
102 000	1.2	1.2	9.07	11.02
227 000	1.15	0.34	27.11	40.45
410 000	1.02	0.14	51.95	73.70

ignored, particularly if sedimentation methods are not available as a check. In such a case, the thickness of the adsorbed layer would be overestimated.

## Experimental Section

**Materials.** Poly(L-lysine) hydrobromide was supplied by Sigma Chemical Co. with an  $M_w/M_n$  ratio between 1.05 and 1.17. The PLL molecular weight was in the range 52 000–410 000 g mol<sup>-1</sup> (Table I). It was dissolved in triply distilled water with no added salt. At the pH value ( $\sim$  7) thus obtained, PLL is essentially an extended coil. Sodium poly(styrene sulfonate) was supplied by Polymer Laboratories with molecular weight 400 000 and  $M_w/M_n = 1.1$ . Since all the solutions were prepared in the absence of any added salt, their ionic strength varied with polymer concentration. This point will be further discussed below. Triton X-100 (poly(ethylene glycol)-*p*-isooctyl phenyl ether) was supplied by Aldrich Chemical Co. and added to the particle suspension (where indicated) up to a concentration of 0.01%. Weakly negatively charged polystyrene spheres (surface charge density 0.004 mequiv/g  $\approx$  0.43  $\mu\text{C cm}^{-2}$  for the particles of diameter 64 nm according to the manufacturer's data) were obtained from Metachem Diagnostics and Agar Scientific Co. with radii of  $32 \pm 9$ ,  $49 \pm 3$ , and  $65 \pm 15$  nm as determined by transmission electron microscopy and photon correlation spectroscopy. Particle sizes and adsorbed layer thicknesses were also checked by using both a sedimentation method and a Malvern System 4700c submicron particle analyzer. The smallest readily observable volume fraction of particles was used in all experiments in order to minimize interparticle interactions; for sedimentation, this was  $1.0 \times 10^{-3}$  for the 32-nm probes, and  $5.0 \times 10^{-4}$  for the 49- and 65-nm probes, and  $1.0 \times 10^{-4}$  for all probes in the light-scattering experiments. Samples were prepared by the careful addition of polymer solution to a suspension of the polystyrene particles in water.

**Sedimentation.** Sedimentation experiments were performed in a Beckman Model E machine equipped with Schlieren optics and an RITC temperature measuring facility. All sedimentation coefficients were corrected to 25 °C. (Further details may be obtained from ref 13.) Different rotor speeds were used between 10 000 and 50 000 rpm and gave identical results within experimental error. It was assumed that sedimentation of the polymer could be neglected at these speeds (its sedimentation coefficient was found to be  $\sim$  2% of that of the particles at 50 000 rpm, although more significant sedimentation was found to occur at 60 000 rpm<sup>13</sup>) and that sedimentation of the particles was through a uniform solvent at rest. To obtain the sedimentation coefficient of the bare latex particles, free from charge effects, the sedimentation was studied in 0.01 M NaCl over a range of latex concentrations. The coefficients varied slowly and linearly with concentration, and the value obtained by extrapolation to zero latex amount was taken as the coefficient in the absence of polyelectrolyte.

Macroscopic polymer solution viscosities were measured by using an Ostwald viscometer in a thermostated water bath at 25 °C. Values of  $C^*$  were estimated from the intercepts of Fuoss<sup>26</sup> plots of  $C/\eta_{sp}$  versus  $C^{1/2}$  to be 2.39, 1.20, 0.34, and 0.14 g/L for PLL of molecular weights 52 000, 102 000, 227 000, and 410 000, respectively, under conditions of zero added salt (see Table I). For NaPSS,  $C^*$  was found to be 0.15 g/L.

**Photon Correlation Spectroscopy.** The instrument used in this study is described in detail by Godfrey et al.<sup>28</sup> The light source was a single-frequency Spectra-Physics 15-mW Model 124A He–Ne laser. The horizontally scattered light was detected by a photomultiplier (EMT 9863) at 90° with respect to the

Table II  
Contribution of Polyelectrolyte to Total Ionic Strength

	ionic strength at concn/g L <sup>-1</sup>				
	1	5	10	15	20
PLL	0.004	0.018	0.036	0.054	0.072
NaPSS	0.004	0.02	0.041	0.062	0.082

incident beam. Specially shaped and positioned baffles were used to cut down stray light. The signal from the photomultiplier was led via a Malvern amplifier-discriminator (RR63) to the Malvern correlator (K7025). Digital output from the correlator was stored on a floppy disk and eventually processed on an IBM 3084 computer. The homodyne intensity autocorrelation function  $g^2(\tau)$  was measured at  $25 \pm 0.02^\circ\text{C}$ . The data were analyzed by using the method of cumulants to determine the diffusion coefficient of the probe particles.

**Analysis of Results.** The relative viscosity experienced by the probe particles moving through the polymer solution is calculated from the sedimentation equation

$$S = \frac{2(\rho_p - \rho_s)R^2}{9\eta} \quad (5)$$

where  $S$  is the sedimentation coefficient,  $\rho_p$  and  $\rho_s$  are the densities of the particle and solvent, respectively,  $R$  is the radius of the particle, and  $\eta$  is the solution viscosity. The calculated relative viscosity experienced by the particles ( $\eta_c$ ) is thus equal to

$$\eta_c = \frac{\eta_s}{\eta_o} = \frac{(\rho_p - \rho_s)S_o}{(\rho_p - \rho_o)S_s} \sim \frac{S_o}{S} \quad (6)$$

where the subscript  $o$  refers to water. For the light-scattering data,  $\eta_c$  is calculated from the Stokes-Einstein equation (eq 1) as

$$\eta_c = D_o/D \quad (7)$$

where  $D_o$  is the diffusion coefficient in water. Both of the above expressions for  $\eta_c$  invoke the constancy of the probe radius over the range of polymer concentrations examined, which would be expected to be valid as the latter are well above the plateau for adsorption.<sup>21</sup>  $\eta_c/\eta_m = 1$  represents ideal Stokes-Einstein behavior.  $S$  values were usually reproducible to  $\sim \pm 1\%$ , unless aggregation was involved.

**Sedimentation Behavior of Polystyrene Latex Probes in Polyelectrolytes.** Since the latex particles are weakly charged (negatively), their interaction with polyelectrolytes involves electrostatic forces and ionic strength effects. However, the polyelectrolytes (with their counterions) themselves contribute to the total ionic strength to a very significant extent. Since there is strong evidence that counterions are strongly bound,<sup>27</sup> it is assumed below for the point of illustration that both PLL and NaPSS are half-dissociated, and accepting that the charges on the polymer chain are isolated single charges (for the purpose of ionic strength calculations), then the contributions to ionic strength are given in Table II. These estimates are very approximate, ignoring any possible variation in the degree of dissociation with dilution, but must be considered in interpreting the adsorption of PLL and NaPSS on latex spheres.

When PLL of molecular weight 102 000 is added to the smallest probes (at a probe concentration of 1 g/L) at low concentrations ( $< 1$  g/L), the original single peak of the probes in water is transformed into one showing approximately two-thirds of the original peak area, but accompanied by a long, forward extension sedimenting ahead representing a range of aggregated material with sedimentation coefficients of up to 4 or 5 times greater than the main peak. This could well represent the effect of charge neutralization, leading to aggregation. With a further increase in PLL concentration (1–10 g/L), such general aggregation is much reduced, but in most experiments, a well-defined main peak was accompanied by up to 25% of a more rapidly sedimenting material whose sedimentation coefficient was 1.4–1.6 times greater—corresponding to a dimer of the original material. At still higher PLL concentrations ( $> 10$  g/L), the peaks become much less well-defined and spread rapidly, eventually causing the disappearance of a well-defined main component. Such

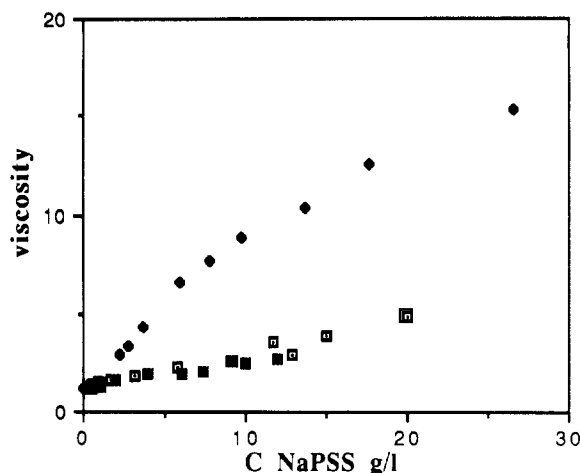


Figure 2. Plot of  $\eta_m$  (□),  $\eta_c$  in the absence of Triton X-100 (◆), and  $\eta_c$  in the presence of 0.01% Triton X-100 for NaPSS using 32-nm PS particles.

behavior was common to each of the PLL's used, although with increased molecular weight, the various PLL concentration ranges mentioned above were lowered. Similar effects were observed with the two larger PS particles, also at modified values of the PLL concentrations.

This paper is concerned with the range of PLL concentrations over which the main peak was well-defined and measurable. In such cases, a plot of  $\ln$  (radial distance) against time was usually accurately linear, but occasionally at the higher PLL concentrations, the slope decreased with increasing radial distance, behavior reminiscent of the sedimentation of dilute aqueous gels<sup>28</sup>—this behavior was not further investigated here.

The addition of NaPSS to the 32-nm radius PS particles was also followed by ultracentrifugation, with quite different results. It should be recalled that no neutralization of charge is involved and no dimer formation occurred. At low concentrations of NaPSS ( $< 10$  g/L), the single sedimenting peak remained well-defined, and  $\ln$  (radial distance) against time was linear. At higher concentrations ( $> 10$  g/L), the peak became broader and eventually tended to break up. With the addition of 0.1 g/L Triton X-100, the boundary remained well-defined as the NaPSS concentration increased, and the plot was always linear.

## Results

**Sedimentation Behavior of Polystyrene Latex Probes in NaPSS.** Figure 2, which refers to the 32-nm PS particles in NaPSS, shows the viscosity data obtained directly ( $\eta_m$ ) on the NaPSS solutions, as well as that calculated ( $\eta_c$ ) by eq 6 from the measured sedimentation coefficients. Data for  $\eta_c$  are given both in the absence and the presence of 0.01% Triton X-100. While in the absence of Triton X-100 the effective viscosity is clearly much higher than that measured directly, it is clear that 0.01% Triton X-100 restores the effective viscosity values almost completely to that ( $\eta_m$ ) directly measured. Figure 3 expresses the same data in terms of deviations from Stokes-Einstein behavior. The shape of this curve is very similar to that for data obtained with PEO in the absence of Triton X-100 in a previous study.<sup>14</sup> In separate experiments using both dynamic light-scattering and sedimentation velocity measurements (to be published), the thickness of the Triton X-100 adsorbed layer on the 32-nm particles was found to be  $\sim 1$  nm. On the other hand, the thickness of the adsorbed NaPSS layer over the range 0.095–1.14 g/L NaPSS was found to be  $\sim 10$  nm. (However, it should be noted that the light-scattering data tended to be very scattered and by its very nature are likely to give misleading results when aggregation is present.)

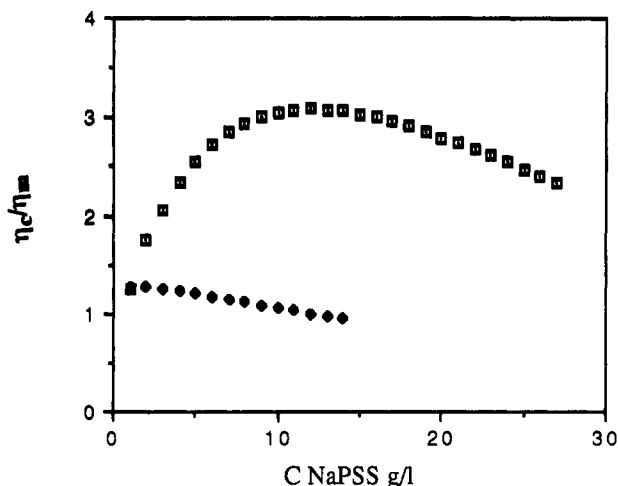


Figure 3.  $\eta_c/\eta_m$  for NaPSS with ( $\blacklozenge$ ) and without ( $\square$ ) Triton X-100, determined from sedimentation measurements of the 32-nm PS particles.

**Sedimentation Rates of the 32-nm PS Particles in PLL Solutions.** Figure 4 shows the plot of  $\eta_c/\eta_m$  against PLL concentration for the 32-nm probes measured via sedimentation in PLL solutions of the four molecular weights. It can be seen that the general shape of the curves is the same for all PLL molecular weights (but very different from the NaPSS data). The ratio initially falls below unity until a broad minimum value is reached at a concentration  $C_{\min}$ , after which it rises steeply. The depth of the minimum increases with increasing PLL molecular weight. Table I includes some features of these curves as a function of molecular weight. If the data are plotted in terms of  $\ln(C/C^*)$  (Figure 4e), the similarity of shapes between the curves again shows up, but it is clear that scaling arguments (which predict that  $C/C^*$  will be the operative parameter beyond  $C^*$ ) do not apply:  $C_{\min}$  does not occur at a constant value of  $C/C^*$ , but instead moves to higher values as the molecular weight increases.

Figure 5 shows a plot of  $\eta_c/\eta_m$  versus  $\ln(C/C^*)$  for the 32-nm probes from the light-scattering data. The general shape of the curves above  $C^*$  is similar to that observed in sedimentation, i.e., an initial decrease in  $\eta_c/\eta_m$  followed by a sharp increase, except that the curves are shifted to lower concentrations. The data below  $C^*$  are rather scattered, and this may be due to the occurrence of aggregates that although present at a low relative concentration, nevertheless dominate the scattering. It should be recognized that in sedimentation such aggregates are deliberately neglected. As was found for sedimentation, the highest molecular weight polymer shows the greatest deviations from Stokes-Einstein behavior.

**Variation of Probe Size for PLL of Molecular Weight 410 000.** In order to determine the effect of probe size on the point at which the microviscosity increases, the sedimentation behavior of the different polystyrene latices was investigated. Figure 6 shows a plot of  $\eta_c/\eta_m$  versus PLL concentration for the three particles for both sedimentation and light-scattering data. It can be seen that the negative deviations from Stokes-Einstein behavior are greatest for the smallest particles and that the sharp increase in apparent viscosity occurs at higher polymer concentrations for these particles (Table III).

## Discussion

The behavior of the probe particles in NaPSS solutions will first be considered. The similarities between the upper curves in Figure 3 (i.e., in the absence of Triton X-100)

and Figure 1 suggest that a similar mechanism must be operating. The explanation for  $\eta_c/\eta_m$  being greater than 1 in the PEO case<sup>14</sup> lies in the adsorbed PEO layer: long tails (which will be most pronounced for high molecular weight material) interacting with the polymer in solution, leading to an effective increase in microviscosity above that of the bulk solution viscosity. Although at first sight it may seem surprising that a polyelectrolyte should adsorb with tails extending into solution, this was found previously<sup>24</sup> for NaPSS adsorbing onto weakly charged PS particles from a light-scattering study, the measured layer thicknesses from this earlier study being  $\sim 40$  nm for a 74 000 molecular weight sample and  $\sim 160$  nm for a molecular weight of 780 000. However, noting the problems discussed earlier regarding aggregation, these values may be an overestimate. In addition, the data on the hydrodynamic layer thickness measured at only low concentrations cannot be considered an adequate guide to the layer thickness at substantially higher concentrations, as will be discussed in more detail with reference to the PLL results.

As the NaPSS concentration is increased, it is clear that ultimately the probe particle must respond as to a continuum, in which case the Stokes-Einstein equation will be approached. Thus, there must be a fall off in the ratio  $\eta_c/\eta_m$  at sufficiently high concentrations, and this decrease is seen beyond  $C \sim 11$  g/L in Figure 3. That in the presence of Triton X-100 the ratio  $\eta_c/\eta_m$  is very close to 1 lends additional support to the idea that it is the adsorbed polymer layer (which will be suppressed by the presence of Triton X-100) that is leading to the deviations from Stokes-Einstein behavior. In this sense, the measured diffusion cannot strictly be described as "probe diffusion" since the probe is not inert.

The behavior of the PLL solutions is clearly more complex and cannot immediately be described within the same framework. However, as will become apparent, we believe that the adsorbed layer is still the pertinent feature in explaining the results. In the absence of salt and at low concentrations, PLL is a relatively stiff molecule because of the charges along the chain. In this configuration, it will adsorb predominantly without tails. By adding salt, screening of these charges occurs so that the molecule becomes more flexible. However, an increase in the segment density achieved by adding more polymer (even in the absence of salt) will also encourage screening<sup>29,30</sup> and can therefore lead to enhanced flexibility. As the flexibility increases, the molecule will approximate more closely to a neutral polymer and would therefore be expected to adsorb in a state with more tails being present and hence also a greater hydrodynamic radius. Since the concentration at which the molecule can no longer be regarded as a stiff chain has been suggested to scale in the bulk as<sup>29</sup>

$$C_p \sim 1/l_B^2 b M^2 \quad (8)$$

where  $l_B$  is the Bjerrum length and  $b$  the monomer length (both of which will typically be a few angstroms), it is clear that the increased flexibility will set in at a lower concentration for high molecular material than for low. In addition, the length of the tails will be greater for the high molecular weight polymer. (It should be noted that it is thought that screening by counterions is rather inefficient.<sup>30</sup>)

With these ideas in mind, we now return to a consideration of Figure 4. At low polymer concentration, the chain is stiffened by its charges and adsorbs in a rather

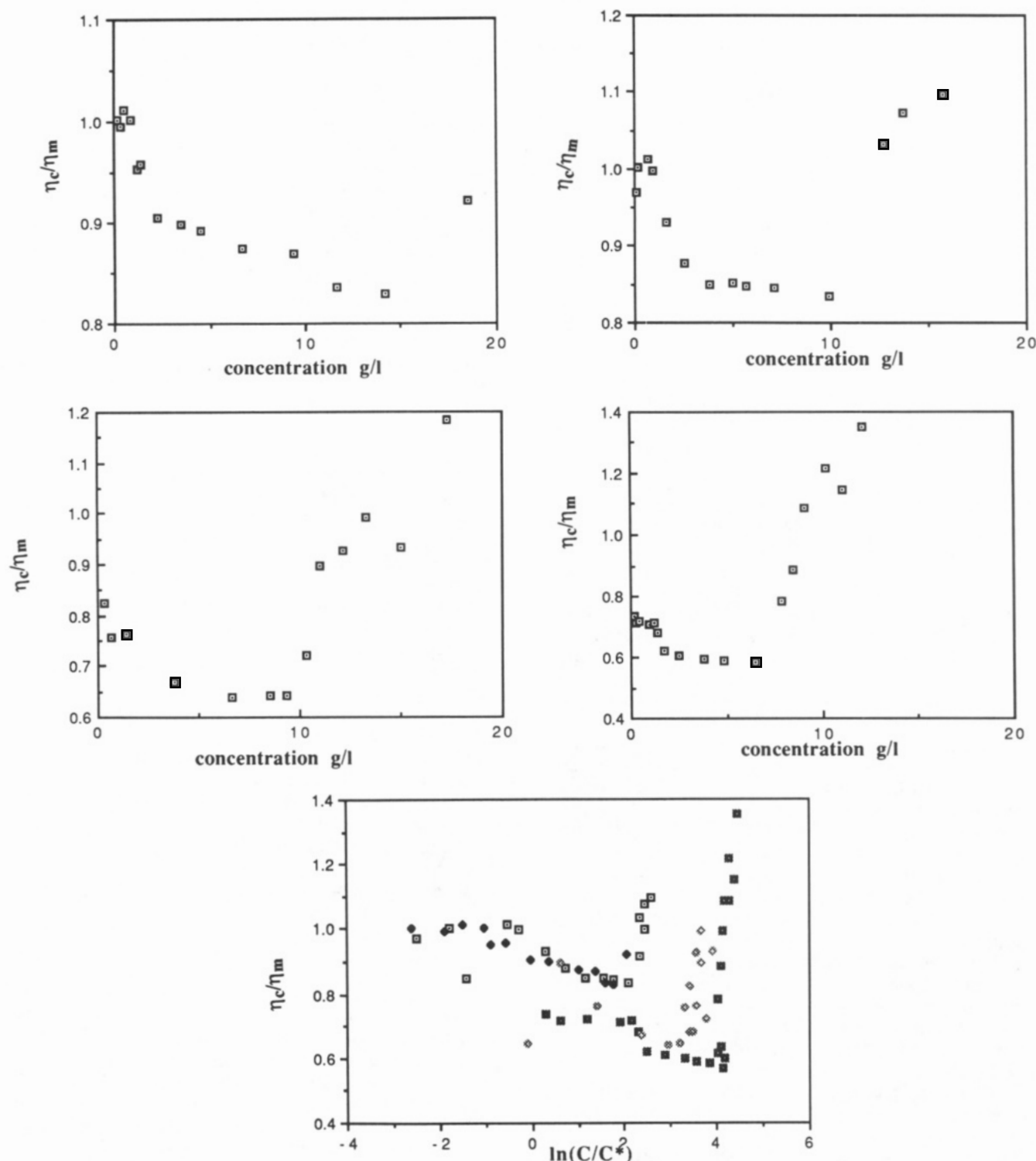


**Figure 4.**  $\eta_c/\eta_m$  determined from sedimentation measurements using the 32-nm PS particles, for PLL of molecular weight (a, top left) 52 000, (b, top right) 102 000, (c, middle left) 227 000, and (d, middle right) 410 000. (e, bottom) The same data for all four molecular weights plotted in terms of the natural logarithm of  $C/C^*$ : ( $\square$ ) 52 000, ( $\blacklozenge$ ) 102 000, ( $\blacksquare$ ) 227 000, and ( $\diamond$ ) 410 000.

flat configuration on the negative latex surface. The behavior of the PS particle will then resemble that in earlier studies on polyelectrolytes,<sup>2-6,8-12</sup> and the particles will move faster than the macroscopic viscosity would imply, leading to  $\eta_c/\eta_m$  being less than unity. However, at a certain concentration, screening of each chain by the others becomes important. The molecule loses stiffness and the adsorption occurs with some tails reaching out into the solution. Eventually the behavior of the particle starts to resemble that of one with a thick adsorbed layer such as occurs for PEO,<sup>14</sup> and the particle is now retarded. Hence, there is a minimum in the  $\eta_c/\eta_m$  plot followed by an upturn.

A similar change in the nature of the adsorbed conformation of PLL has been noted as a function of the Debye screening length (in this case altered by adding salt) by using the surface forces technique,<sup>31</sup> with the adsorbed layer extending much further into solution at high ionic strengths than at low. This confirms the idea that a conformational change in the bulk solution can also be reflected in the adsorbed layer. The steepness of the gradient beyond  $C_{\min}$  suggests that the transition is fairly abrupt, so that once the stiffness has been compromised, the effective hydrodynamic thickness of the particle changes substantially over a narrow concentration range.

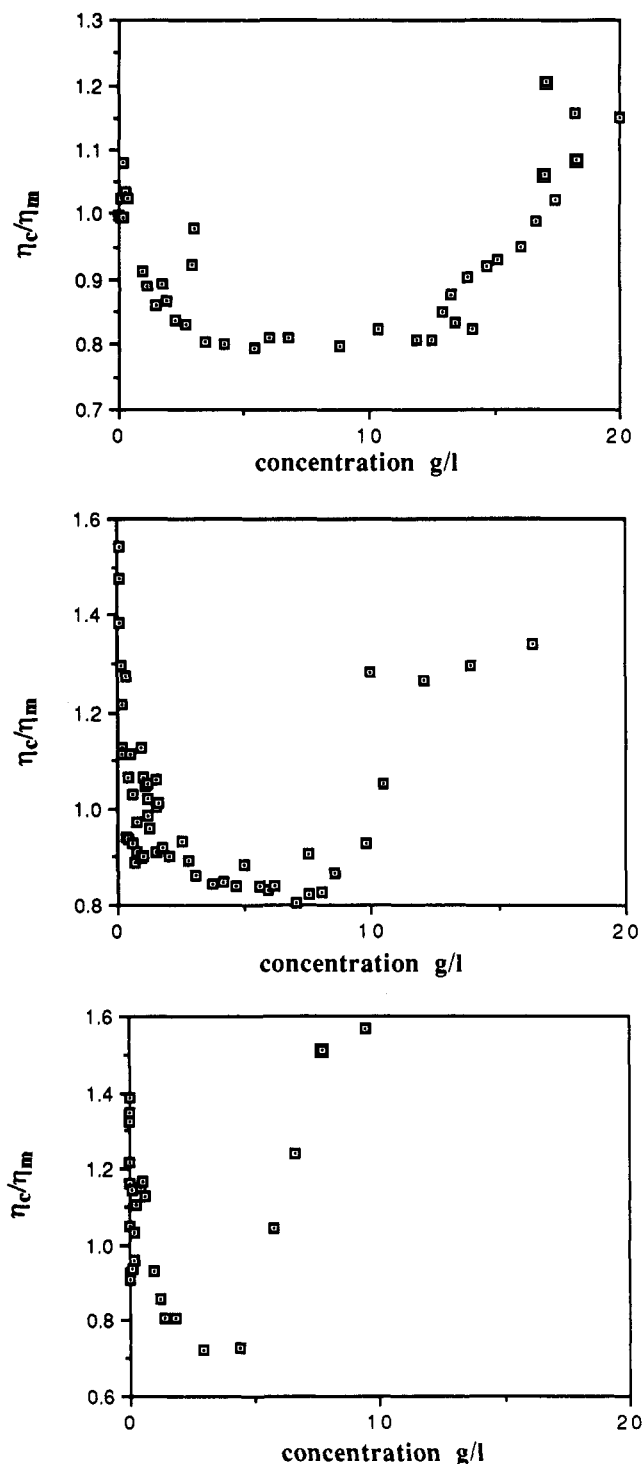


**Figure 5.**  $\eta_c/\eta_m$  determined from light-scattering measurements using the 32-nm PS particles, for PLL of molecular weight (a, top) 52 000, (b, middle) 102 000, and (c, bottom) 227 000.

That the plot of Figure 4e does not yield a universal curve can be understood, since eq 8 predicts a strong molecular weight dependence for the concentration at which stiffness is lost. However, the data for  $C_{\min}$  do not support the form of eq 8; rather  $C_{\min}$  scales approximately as  $M^{1/3}$ . Although it is almost certainly incorrect to assume that  $C_{\min}$  can be identified precisely with the concentration at which the conformational transition occurs, a very different value of the exponent appears to cast doubt on the functional form of the equation.

A further point to address is why the value of  $C_{\min}$  should be lower for the light-scattering data of Figure 5 than that obtained from sedimentation. This discrepancy probably

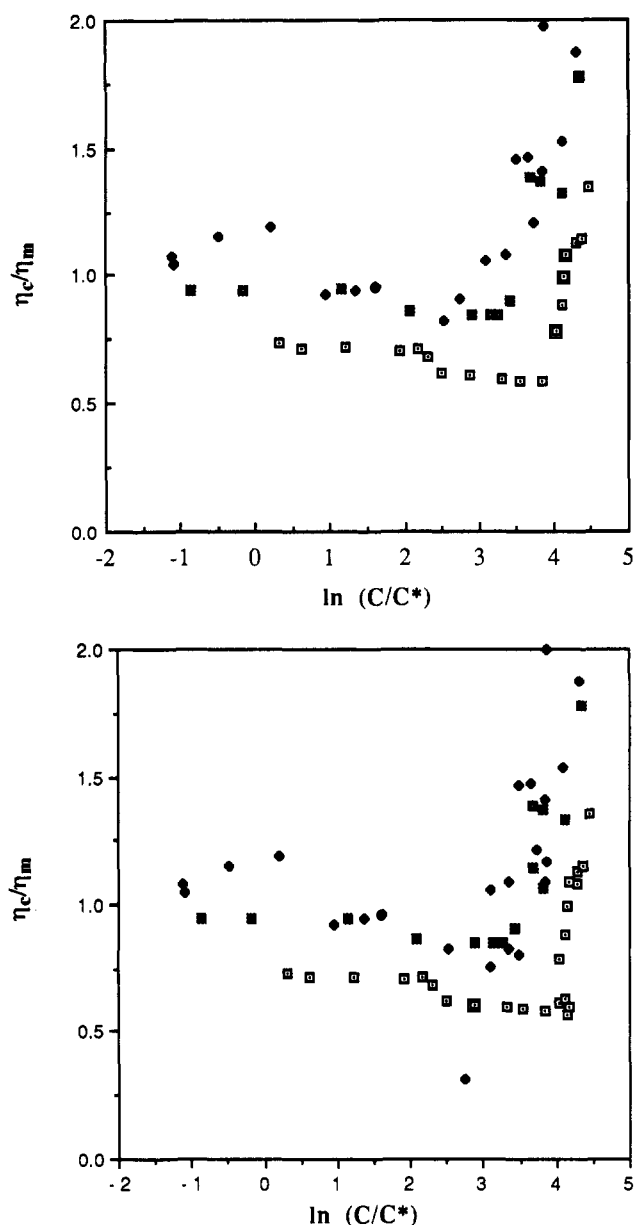


**Figure 6.**  $\eta_c/\eta_m$  determined for PLL of molecular weight 410 000, for the 32-nm ( $\square$ ), 49-nm ( $\blacklozenge$ ), and 65-nm ( $\blacksquare$ ) PS particles, plotted against the natural logarithm of  $C/C^*$ : (a, top) from sedimentation and (b, bottom) from light-scattering measurements.

**Table III**  
Effect of Probe Radius on  $\eta_c/\eta_m$  for PLL of Molecular Weight 410 000

probe radius/nm	$C$ (in g L <sup>-1</sup> ) at min in $\eta_c/\eta_m$		$C$ (in g L <sup>-1</sup> ) at $\eta_c/\eta_m = 1$	
	sedimentation	LS	sedimentation	LS
32	6.5	6.9	8.7	9.6
49	1.8	2.6	4.0	4.0
65	2.5	3.8	4.6	4.9

arises from the difficulty of correctly allowing for polydispersity in the light-scattering case; not allowing for aggregates will have the effect of leading to an underestimate of  $D$  and hence an overestimate of  $\eta_c$ . This would then lead to the depth of  $C_{\min}$  being less than for the sedimentation measurements, although the trends are the same.

Figure 6 shows the effect of different particle sizes. The behavior of the two larger particles is very similar, with  $C_{\min}$  occurring at very much the same concentration. The upturn in the  $\eta_c/\eta_m$  ratio is delayed to significantly higher

concentrations for the smallest particles. A similar upward shift in concentration for the occurrence of maximum effect of tails following adsorption of PEO upon small particles has been observed previously<sup>14</sup> and was attributed to the effect of the radius of curvature of the particles upon the configuration of adsorption: steric hindrance may affect the adsorption segment density even when the polymer is in the flexible configuration.

A frequently used approach to looking at probe diffusion is to use a stretched exponential.<sup>8</sup> Translating eq 2 to the form appropriate for sedimentation leads to

$$S/S_0 = \exp(-BC^\nu)$$

where  $B = AR^\delta$ . The data can be fitted in this way, but since the operative physical principles change with concentration, there seems to be no real justification for proceeding like this, although the fits obtained appear quite reasonable and lead to a value of  $\nu$  of close to 0.5, which has been predicted by theory.<sup>32</sup>

### Conclusions

The diffusion of PS latices through solutions containing NaPSS and PLL has been examined. For NaPSS, it is found that the behavior is broadly similar to that of the neutral polymer PEO due to the presence of an adsorbed layer with tails that reach into the solution. These tails effectively increase the local polyelectrolyte concentration, and hence, the local viscosity experienced by the diffusing particle is larger than that measured macroscopically. For PLL, the motion of the particles is more complicated. At low concentrations of polymer, adsorption is in a flat configuration and simply leads to a small increase in effective particle radius. The diffusion or sedimentation over this concentration range is therefore faster than would be expected from Stokes-Einstein behavior, as has been seen previously by various workers for a variety of different polyelectrolytes. However, at higher concentrations, inter-chain screening of the electrostatic interactions between charges leads to increased flexibility of the molecules. The configuration of the adsorbed layer now changes to one in which tails are present, and the particle is slowed down, in a manner similar to that for neutral polymers.

**Acknowledgment.** We are grateful to the AFRC for financial support of this work and to Mr. N. Buttress for

performing the ultracentrifuge experiments.

### References and Notes

- (1) Langevin, D.; Rondelez, F. *Polymer* **1978**, *19*, 875.
- (2) Lin, T. H.; Phillies, G. D. J. *Macromolecules* **1984**, *17*, 1687.
- (3) Lin, T. H.; Phillies, G. D. J. *J. Phys. Chem.* **1982**, *86*, 4073.
- (4) Lin, T. H.; Phillies, G. D. J. *J. Colloid Interface Sci.* **1984**, *100*, 82.
- (5) Ullmann, K.; Ullmann, G.; Lindner, R. M.; Phillies, G. D. J. *J. Phys. Chem.* **1985**, *89*, 692.
- (6) Ullmann, K.; Ullmann, G.; Phillies, G. D. J. *J. Colloid Interface Sci.* **1985**, *105*, 315.
- (7) Phillies, G. D. J.; Ullmann, K.; Ullmann, G.; Lin, T. H. *J. Chem. Phys.* **1985**, *82*, 5242.
- (8) Phillies, G. D. J.; *Macromolecules* **1986**, *19*, 2367.
- (9) Phillies, G. D. J.; Malone, C.; Ullmann, K.; Ullmann, G.; Rollings, J.; Yu, L. *Macromolecules* **1987**, *20*, 2280.
- (10) Gorti, S.; Ware, B. R. *J. Chem. Phys.* **1985**, *83*, 6459.
- (11) Brown, W.; Rymden, R. *Macromolecules* **1986**, *19*, 2942.
- (12) Brown, W.; Rymden, R. *Macromolecules* **1987**, *20*, 2867.
- (13) Nehme, O. A.; Johnson, P.; Donald, A. M. *Macromolecules* **1989**, *22*, 4326.
- (14) Cooper, E. C.; Johnson, P.; Donald, A. M. *Polymer*, in press.
- (15) Edwards, S. F. *Proc. Phys. Soc.* **1966**, *88*, 265.
- (16) de Gennes, P.-G. *Scaling Concepts in Polymer Physics*; Cornell University Press: Ithaca, NY, 1979.
- (17) de Gennes, P.-G.; Pincus, P.; Velasco, R. M.; Brochard, F. *J. Phys.* **1976**, *37*, 1461.
- (18) des Cloizeaux, J. *J. Phys. (Paris)* **1975**, *36*, 281.
- (19) de Gennes, P.-G. *Macromolecules* **1976**, *9*, 594.
- (20) Odijk, T. *Macromolecules* **1979**, *12*, 688.
- (21) Furasawa, K.; Kaneska, M.; Yamashita, S. *J. Colloid Interface Sci.* **1984**, *99*, 341.
- (22) Bonekamp, B. C.; van der Schee, H. A.; Lyklema, J. *Croat. Chem. Acta* **1983**, *56*, 695.
- (23) Cohen Stuart, M. *J. Phys. (Paris)* **1988**, *49*, 1001.
- (24) Cosgrove, T.; Obey, T. M.; Vincent, B. *J. Colloid Interface Sci.* **1986**, *111*, 409.
- (25) Fuoss, R. M.; Strauss, U. P. *J. Polym. Sci.* **1948**, *3*, 603.
- (26) Godfrey, R. E.; Johnson, P.; Stanley, C. J. In *Biomedical Applications of Laser Light Scattering*; Sattelle, D. B., Lee, W. I., Ware, B. R., Eds.; Elsevier Biomedical Press: Amsterdam, 1982; p 373.
- (27) Breuer, M. M. In *Polymer Science*; Jenkins, A. D., Ed.; North Holland: Amsterdam, p 1136.
- (28) Johnson, P. *Proc. R. Soc. London, Ser. A* **1964**, *278*, 527.
- (29) Rabin, Y. *Phys. Rev. A* **1987**, *35*, 3579.
- (30) Witten, T. A.; Pincus, P. *Europhys. Lett.* **1987**, *3*, 315.
- (31) Dix, L. R.; Davies, R. J.; Toprakcioglu, C. *Colloids Surf.* **1988**, *31*, 147.
- (32) Cukier, R. I. *Macromolecules* **1984**, *17*, 252.

**Registry No.** PLL, 25988-63-0; NaPSS, 62744-35-8; polystyrene, 9003-53-6.